

PVP2017-65755

ANALYTICAL SOLUTIONS FOR LIQUID SLUGS AND PIGS TRAVELING IN PIPELINES WITH ENTRAPPED GAS

Arris S. TIJSSELING

Department of Mathematics and Computer Science
Eindhoven University of Technology
P.O. Box 513, 5600 MB Eindhoven
The Netherlands
E-mail: a.s.tijsseling@tue.nl

Qingzhi HOU

School of Computer Science and Technology;
State Key Laboratory of Hydraulic Engineering
Tianjin University
Tianjin 300072
China
E-mail: qhou@tju.edu.cn

Zafer BOZKUŞ

Hydromechanics Laboratory
Department of Civil Engineering
Middle East Technical University
Ankara 06800
Turkey
E-mail: bozkus@metu.edu.tr

ABSTRACT

Liquid slugs have a relatively low mass and can therefore – when they occupy a full cross-section of a pipeline – be accelerated to very high velocities by means of pressurized gas. When entrapped gas pockets are present, pressures and temperatures may become dangerously high. Simple models and analytical solutions are derived and used to predict transient velocities, pressures and temperatures. The models have a generic character as they also describe the basics of breaking surface waves impacting on a wall, and pigs and bullets propelled by compressed gas.

Key words

liquid slug, liquid column, pipe pig, entrapped gas, Bagnold model, mass oscillation, nonlinear spring, analytical solution

INTRODUCTION

Condensates may form in pipelines that carry vapors or condensable gases. These condensates will collect in the lower parts of the system thereby forming (partial) blockages which can be blown away by pressurized gas flowing at high speed.

The condensates may transform to accelerating liquid slugs that impose serious hazard to the system safety. The authors have studied the phenomenon of traveling liquid slugs by experiment and theory [1-3]. Entrapped gas pockets form another danger in pipelines that carry liquids [4-8]. The pockets have the property to store and release energy in agreement with the dynamics of the system. In impacts and other rapid events, the system pressures and temperatures may rise to unacceptably large values. The authors have studied this subject for the event of rapid pipe filling [9-10].

In the present paper the motion of the liquid slug is impeded by trapped gas ahead of it. The slug will eventually bounce back and a mass oscillation is what remains. Analytical solutions are found for 0D (in the sense that the model in fact is a spring-mass system) and 1D (in the sense that the flow is one direction, with a flat-faced traveling liquid front) models. These give useful insight and directly lead to non-dimensional parameters that characterize the problem.

The first model of this kind is by Bagnold (1939) [11] who studied the impact of breaking free-surface water waves on rigid walls. He showed experimentally that entrapped air pockets and accompanying phenomena have a big effect on the wave impact pressures. His simple model described a given mass of water hitting a rigid wall, where a small layer of air (that cannot

escape fast enough) is present. The subject still is of uttermost importance in sloshing liquids [12-15] and for the impact of an irregularly shaped solid body onto the free surface of a liquid or even in the case of perfectly flat impacts [16-18]. Another relevant application is solid capsules [19] and pigs [20-24] driven by (or driving) gas and liquid flows. Yet another application is autoinjectors in medicine [25].

Our study concerns a rigid body (liquid or solid) moving into a confined gas volume. Analytical expressions are derived for the rigid body's velocity from which extreme pressures and temperatures can be calculated. The acoustic effects (gas and water hammer) that occur in extreme cases of impact are ignored herein.

LIQUID SLUG TEST PROBLEM

The theoretical test problem is a liquid slug accelerating from rest towards gas that is trapped at a closed end. Figure 1 is a simple sketch of the situation. Sudden opening of an upstream valve connected to a pressurized gas tank (not shown in Fig. 1) initiates the event. The input data are taken from the parameter variation study presented in [3] and concern a water-air system where the diameter of the horizontal pipe is $D = 0.01$ m and the constant length of the cylinder-shaped water-slug is $L_0 = 3$ m. The air occupies an initial length $L_{\text{gas},0} = 9$ m and has an initial absolute pressure $P_{\text{gas},0} = 1$ bar, so that the pipe length is $x_L = L_0 + L_{\text{gas},0} = 12$ m. The absolute pressure in the air-tank is $P_{R,0} = 6$ bar, the specific gas constant for air is $R = 287$ m²/(s² K), and the polytropic coefficient n is either 1 or 1.4 herein. The skin friction coefficient for the slug flow is $f = 0.016$. The liquid slug and air pocket have initial masses of 0.24 kg and 0.85 g, respectively. The mass density of the water is $\rho = 1000$ kg/m³, and the initial air density is taken equal to $\rho_{\text{gas},0} = 1.2$ kg/m³, which corresponds to an initial temperature $T_{\text{gas},0} = 290$ K. The gravitational acceleration is $g = 9.81$ m/s², but it is not an input parameter when the pipe is horizontal ($\theta = 0$).

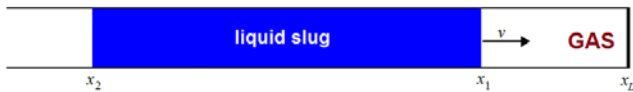


Fig. 1 Sketch of analyzed system with $L_0 = x_1 - x_2$ and $\theta = 0$.

GOVERNING EQUATIONS

The mathematical model is that of a nonlinear spring-mass system with damping due to skin friction. Any acoustic effects – that is wave propagations – are ignored: the slug is rigid with planar front and tail, and the gas is ideal and uniform. There is no hold-up and pick-up of liquid so that the slug does not break down and has infinite life time. The governing equations for

liquid velocity v , liquid front position x_1 , and absolute gas pressure P_{gas} , read [3, 9]:

$$\frac{dv}{dt} = \frac{P_2 - P_{\text{gas}}}{\rho L_0} + g \sin \theta - \frac{f}{2D} v |v| \quad (1)$$

$$\frac{dx_1}{dt} = v \quad (2)$$

$$L_{\text{gas}}^n P_{\text{gas}} = L_{\text{gas},0}^n P_{\text{gas},0} \quad (3)$$

where P_2 is the pressure at position x_2 , θ is the downward inclination of the conduit, and $L_{\text{gas}} = x_L - x_1$, see Fig. 1. The pressure P_2 can be either constant (as $P_{R,0}$ in the slug impact problem) or variable (as in the extended Bagnold model). Substitution of Eq. (3) into Eq. (1) gives

$$\frac{dv}{dt} = F(x_1) - \frac{f}{2D} v |v| \quad (4)$$

where

$$F(x_1) = \frac{P_2}{\rho L_0} - \left(\frac{x_L - x_{1,0}}{x_L - x_1} \right)^n \frac{P_{\text{gas},0}}{\rho L_0} + g \sin \theta \quad (5)$$

is the driving acceleration and $x_{1,0} = L_0 + x_{2,0}$ is the starting position of the slug front.

ANALYTICAL SOLUTIONS

The Eqs. (2) and (4) can be combined such that

$$\frac{1}{2} \frac{dv^2}{dx_1} = v \frac{dv}{dx_1} = v \frac{(dv/dt)}{(dx_1/dt)} = v \frac{dv/dt}{v} = \frac{dv}{dt} = F(x_1) - \frac{f}{2D} v |v|$$

or

$$\frac{dv^2}{dx_1} \pm \frac{f}{D} v^2 = 2F(x_1) \quad (6)$$

which is a linear ODE in terms of $v^2(x_1)$.

For a frictionless system ($f = 0$) the solution is

$$v^2(x_1) - v^2(x_{1,0}) = 2 \int_{x_{1,0}}^{x_1} F(x) dx \quad (7)$$

For $n = 1$ this gives

$$v^2(x_1) - v^2(x_{1,0}) = \frac{2}{\rho L_0} \left[(P_2 + \rho g L_0 \sin \theta)(x_1 - x_{1,0}) - P_{\text{gas},0} (x_L - x_{1,0}) \ln \left(\frac{x_L - x_{1,0}}{x_L - x_1} \right) \right] \quad (7a)$$

and for $n \neq 1$:

$$v^2(x_1) - v^2(x_{1,0}) = \frac{2}{\rho L_0} \left[(P_2 + \rho g L_0 \sin \theta)(x_1 - x_{1,0}) + \left(-\frac{P_{\text{gas},0}}{n-1} (x_L - x_{1,0}) \left(\left(\frac{x_L - x_{1,0}}{x_L - x_1} \right)^{n-1} - 1 \right) \right) \right] \quad (7b)$$

The relation $v^2(x_1)$ describes a symmetrical closed curve (for $f=0$) with $v(x_1) = +\sqrt{v^2(x_1)}$ for forward flow and $v(x_1) = -\sqrt{v^2(x_1)}$ for backward flow.

For the liquid slug moving into the gas pocket ($v > 0$) and with friction ($f > 0$) the solution is

$$v^2(x_1) - v^2(x_{1,0}) e^{-\frac{f}{D}(x_1 - x_{1,0})} = 2 e^{-\frac{f}{D}x_1} \int_{x_{1,0}}^{x_1} e^{\frac{f}{D}x} F(x) dx \quad (8a)$$

with $v(x_1) = +\sqrt{v^2(x_1)}$. For $n = 1$ [in $F(x)$] this leads to a symbolic solution in terms of exponential integrals. See Appendix A. For $n \neq 1$ the symbolic solution contains incomplete gamma functions. Of course, the integral in Eq. (8a) can easily be calculated numerically.

For the liquid slug moving away from the gas pocket ($v < 0$) and with friction ($f > 0$) the solution is

$$v^2(x_1) - v^2(x_{1,00}) e^{\frac{f}{D}(x_1 - x_{1,00})} = 2 e^{\frac{f}{D}x_1} \int_{x_{1,00}}^{x_1} e^{-\frac{f}{D}x} F(x) dx \quad (8b)$$

with $v(x_1) = -\sqrt{v^2(x_1)}$ and where $x_{1,00}$ is the position of the slug front when it reverses direction for the first time, that is at maximum x_1 , minimum L_{gas} and maximum P_{gas} . The function $v(x_1(t))$ becomes double-valued after the first flow reversal at $v(x_1(t)) = 0$ and spirals towards the equilibrium point.

Bagnold model

The Bagnold model [11] is a special case where there is no friction, no gravity, no driving acceleration, but an initial velocity $v(x_{1,0}) = v_0 > 0$. Thus $f=0$, $g=0$, $\theta=0$, $P_2 = P_{\text{gas},0}$.

For $n = 1$ this gives

$$v^2(x_1) = v_0^2 - \frac{2P_{\text{gas},0}}{\rho L_0} \left[(x_1 - x_{1,0}) - (x_L - x_{1,0}) \ln \left(\frac{x_L - x_{1,0}}{x_L - x_1} \right) \right] \quad (9a)$$

and for $n \neq 1$:

$$v^2(x_1) = v_0^2 + \frac{2P_{\text{gas},0}}{\rho L_0} \left[x_1 - x_{1,0} - \frac{x_L - x_{1,0}}{n-1} \left(\left(\frac{x_L - x_{1,0}}{x_L - x_1} \right)^{n-1} - 1 \right) \right] \quad (9b)$$

These solutions are exactly those derived by major Bagnold [11].

Extended Bagnold model

The extended Bagnold model [12, 29] is a special case where there is no friction, but gravity (not necessarily in the vertical direction), and there is gas (not necessarily the same) trapped upstream and downstream of the liquid slug as sketched in Fig. 2. Thus $f=0$, $g \neq 0$, $\theta \neq 0$, $v(x_{1,0}) = v_0 \geq 0$. The relation $L_{2,\text{gas}} P_{2,\text{gas}} = L_{2,\text{gas},0}^n P_{2,\text{gas},0}$ with $L_{2,\text{gas}} = x_2 = x_1 - L_0$ is an additional equation analogue to Eq. (3). The slug oscillates in between two gas pockets entrapped in a closed tube. In [12, 29] the liquid slug is elastic. Herein the liquid slug is rigid and exact solutions can be obtained just as in the single-pocket case. These solutions are derived in Appendix B. The equilibrium pressure (obtained from $P_1 = P_2 + \rho g L_0 \sin \theta = P_{\text{eq}}$ and two times Eq. 3)

is

$$P_{\text{eq}} = \left(\frac{P_{1,0}^{1/n} L_{1,0} + P_{2,0}^{1/n} L_{2,0}}{L_{1,0} + L_{2,0}} \right)^n \quad (10a)$$

The corresponding equilibrium length of the ‘‘upstream’’ gas pocket is

$$L_{1,\text{eq}} = \frac{L_{1,0} + L_{2,0}}{1 + \left(\frac{P_{2,0}}{P_{1,0}} \right)^{1/n} \left(\frac{L_{2,0}}{L_{1,0}} \right)} \quad (10b)$$

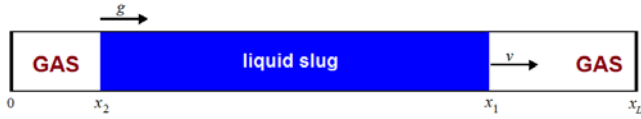


Fig. 2 Sketch of extended Bagnold model with $L_0 = x_1 - x_2$ and $\theta = \pi/2$.

Pig motion

A simple model for pig motion is obtained when the liquid slug is conceived of as a solid body sliding along the pipeline, with a different friction term in Eq. (1). The pig is driven by the pressure difference across it. Assuming that the pig travels long distances, one further assumption is made, namely that the pig length is relatively small: $L_0 \ll L_{1,\text{gas}}$ and $L_0 \ll L_{2,\text{gas}}$, so that $x_L = L_1 + L_2$. Pig control and stabilization is an issue. The simple situation with closed ends shown in Fig. 2 is considered to recognize how fast a pig comes to rest from a non-equilibrium position. The pig has mass m , velocity v , ignored length, and experiences linear friction c with the pipe wall. The governing equations in terms of first derivatives are

$$\frac{dv}{dt} = \frac{P_2 - P_1}{m} A + g \sin \theta - \frac{c}{m} v \quad (11a)$$

$$\frac{dP_1}{dt} = + \frac{n P_1 v}{L_1} \quad (11b)$$

$$\frac{dP_2}{dt} = - \frac{n P_2 v}{L_2} \quad (11c)$$

$$\frac{dL_1}{dt} = -v \quad (11d)$$

$$\frac{dL_2}{dt} = +v \quad (11e)$$

where A is the cross-sectional pipe area, and P_1 , L_1 and P_2 , L_2 are gas pressures and lengths “downstream” and “upstream” of the pig, respectively. Equation (11b) follows from Eq. (11d) and

$$\text{the relation } \frac{d(L_1^n P_1)}{dt} = L_1^n \frac{dP_1}{dt} + n L_1^{n-1} P_1 \frac{dL_1}{dt} = 0.$$

Analytical solutions of Eqs. (11) have not been found for $f \neq 0$, because – strange enough – the friction term is linear instead of quadratic. Numerical time integration using the explicit Euler method is the easiest option, although not the most accurate one.

The Eqs. (11) can be combined into one second-order ODE for L_1 ($\theta = 0$):

$$-m \frac{d^2 L_1}{dt^2} = \left(\frac{P_{2,0} L_{2,0}^n}{(x_L - L_1)^n} - \frac{P_{1,0} L_{1,0}^n}{L_1^n} \right) A + c \frac{dL_1}{dt} \quad (12a)$$

and its linearization for small values of $\xi = L_1 - L_{1,0}$:

$$m \frac{d^2 \xi}{dt^2} + c \frac{d\xi}{dt} + \left(\frac{n P_{1,0} A}{L_{1,0}} + \frac{n P_{2,0} A}{L_{2,0}} \right) \xi = (P_{1,0} - P_{2,0}) A \quad (12b)$$

Equation (12b) represents a spring-mass-damper system with mass m , damping c , and stiffness $k = n A \left(\frac{P_{1,0}}{L_{1,0}} + \frac{P_{2,0}}{L_{2,0}} \right)$. Its

period of undamped free oscillation is $\tau = 2\pi \sqrt{\frac{m}{k}}$. Special cases include $f = 0$, $P_{1,0} = 0$ (vacuum) and $L_{1,0} = \infty$.

Pigs

Pigs (pipeline inspection gauges) are used for the internal cleaning and inspection of pipelines [20-24] and for the removal of condensates. They sometimes produce an audible sound similar to that of a screaming pig. They can be self-propelling or flow-driven. Conversely, capsules or trains in tunnels drive the flow [19]. When modelling pigs in pipelines, it is necessary to allow for non-uniform pipe cross-section and for debris driven ahead of the capsule. The current model is therefore too simple for practical applications.

Too short or too long gas pockets

When the gas pockets become very small ($L_{\text{gas}} \ll D$), the limit of the current model is reached. First of all, unrealistically high temperatures may occur, with values according to the ideal gas law:

$$T_{\text{gas}} = \frac{P_{\text{gas}}}{R \rho_{\text{gas}}} \quad \text{with} \quad \frac{\rho_{\text{gas}}}{\rho_{\text{gas},0}} = \frac{L_{\text{gas},0}}{L_{\text{gas}}} \quad (13)$$

Second, when the stiffness of the gas pocket becomes of the order of the stiffness of the liquid slug, that is

$$\frac{n P_{\text{gas}} A}{L_{\text{gas}}} \approx \frac{K^* A}{L_0} \quad \text{or} \quad \frac{\rho a^2}{\rho_{\text{gas}} a_{\text{gas}}^2} \frac{L_{\text{gas}}}{L_0} \approx 1 \quad (14)$$

water hammer will occur [12-13, 26-29] depending on the different time and length scales. The effective bulk modulus K^* of the liquid includes the hoop elasticity of the pipe wall. Relation (14) corresponds to the dimensionless number δ defined and

investigated in [27]. Third, the assumption of a relatively planar slug front (compared to L_0 and L_{gas}) is violated when

$$\frac{w}{L_{\text{gas}}} \approx 1 \quad (15)$$

where w is the width of the front. This is of particular importance for breaking waves hitting a vertical wall [11] and for flat impacts of solid bodies onto a liquid free-surface [16-18]. Fourth, the validity of the ideal gas law itself becomes questionable. For long gas pockets, gas hammer [30] should be modeled as in [1, 12, 21-24, 28]. This again has to do with multi-scales: the acoustic wave travel time in the gas compared to the convective travel time of the slug.

Work and energy

The liquid slug or pig acts as a piston that compresses the gas. Work and energy relations give useful insight [8, 12], but these are not pursued herein.

NUMERICAL SOLUTION

All governing equations can be reformulated into one autonomous first-order ODE similar to Eqs. (11), that is

$$\frac{dy}{dt} = f(y), \quad \text{with } y := \begin{pmatrix} v \\ P_1 \\ P_2 \\ L_1 \\ L_2 \end{pmatrix} \quad (16)$$

The explicit Euler method has been used to solve Eq. (16) with a numerical time step $\Delta t = 1$ ms for all simulations herein.

RESULTS

Liquid slug impact

The laboratory experiment reported in [31] concerns the impact of an accelerated water slug with a miter bend. The current test problem concerns the impact with compressed gas trapped at a dead end at the location of the bend. The pipe diameter is taken ten times smaller than in [31] to enhance the effect of friction and $\theta = 0$. The calculated slug velocity as function of its front position is shown in Fig. 3a for $n = 1.4$. The slug accelerates from rest and is impeded in its motion by increasing friction and rising gas pressure. Only one flow reversal is shown, because – in reality – the slug is likely to break down when it bounces onto the gas pocket. The 1D model

with two planar fronts and no hold-up becomes questionable when the slug changes direction. The theoretical oscillation is around the equilibria $P_{\text{gas,eq}}$ and $L_{\text{gas,eq}}$:

$$P_{\text{gas,eq}} = P_2 + \rho g L_0 \sin(\theta) \quad \text{and} \quad L_{\text{gas,eq}} = \left(\frac{P_{\text{gas},0}}{P_{\text{gas,eq}}} \right)^{\frac{1}{n}} L_{\text{gas},0} \quad (17)$$

with values of 6 bar ($P_{R,0}$) and 2.5 m (Eq. 17), respectively. The maximum pressure is 8.2 bar and the minimum pocket length is 2.0 m, so that the maximum temperature is 256 °C according to formula (13). From Fig. 3a it is evident that the analytical solution (8) is correct, because it overlaps the numerical solution. The strong influence of friction is clear from the comparison with the $f = 0$ result, which is given as reference solution. Figure 3b shows the pressure build-up in time and the overshooting of the equilibrium pressure by 37%.

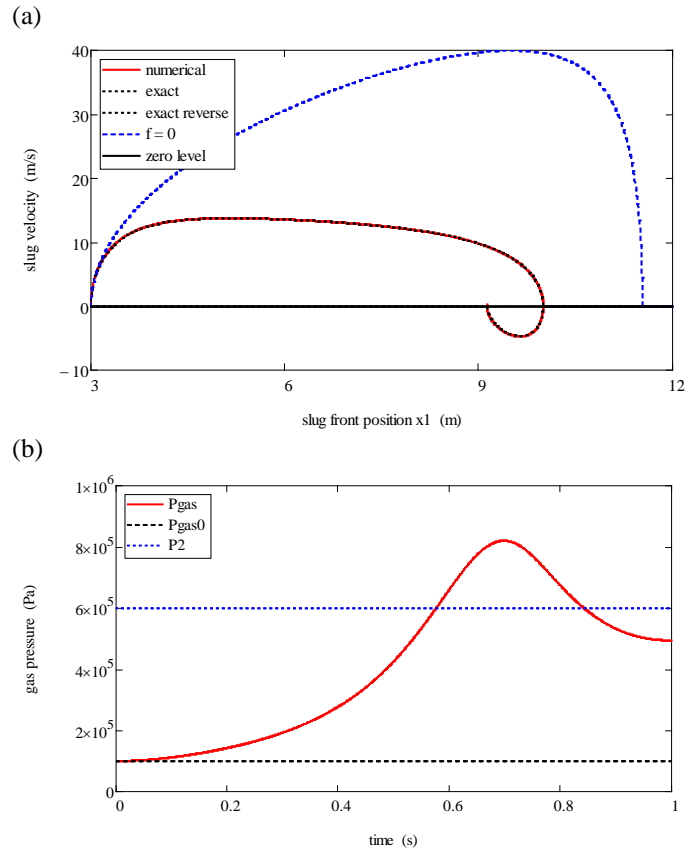


Fig. 3 Liquid slug impact: (a) slug velocity versus position; (b) gas pressure versus time.

Bagnold model

The Bagnold model [11] is tested for $v_0 = 40$ m/s and $n = 1.4$. As stated before: $f = 0$, $g = 0$, $\theta = 0$ and $P_2 = P_{\text{gas},0}$. The dimensionless Bagnold or impact number defined in [12] is based on a non-zero initial velocity:

$$S_B = \frac{\rho v_0^2 L_0}{P_{\text{gas},0} L_{\text{gas},0}} \quad (18)$$

and follows directly from the symbolic solution if it is made dimensionless [Eq. (9) with $x_L - x_{1,0} = L_{\text{gas},0}$]. For $S_B > 8$ water hammer in the slug becomes of significance and for $S_B > 200$ it dominates [12]. Here $S_B = 5.3$ so that we have a rather extreme impact, which is confirmed by a calculated maximum pressure of 22 bar (Eq. 9b) and a maximum temperature of 730 °C (Eq. 13).

Adding friction ($f > 0$) to the model allows introduction of the dimensionless friction-volume parameter or Martin number [4] defined by

$$S_M = \frac{f V_{\text{gas},0}}{D^3} = \frac{\pi f L_{\text{gas},0}}{4 D} = \frac{\pi f (x_L - x_{1,0})}{4 D} \quad (19)$$

where the latter two formulas hold for circular cross-sections and where $x_L - x_{1,0}$ is the maximum distance that can be travelled by the slug. The factor $\pi/4$ may be taken 1 for convenience; formula (19) is then consistent with the expressions in the symbolic solution Eq. (8a).

The extended Bagnold model [12] is similar to the bouncing pig considered in the next paragraph.

Bouncing pig

Instead of the liquid slug, a small copper cylinder is taken with mass $m = 20$ gram which corresponds to a length of about 3 cm when its diameter is just less than $D = 0.01$ m. This “pig” is driven into the closed pipe by 1 liter of compressed air ($P_{2,0} = 2$ bar) behind it. This 1 liter is contained in an “upstream” pipe of length $L_{2,0} = 12.7$ m. As before, $L_{1,0} = x_L = 9$ m, $P_{1,0} = 1$ bar, $T_{1,0} = 290$ K and $\theta = 0$. The resistance coefficient for the pig is $c = 0.1$ kg/s and $n = 1$. The system is like an air gun with a solid bullet. The equilibrium pressure P_{eq} (for $n = 1$) is (Eq. 10a): $P_{\text{eq}} = (P_{1,0} L_{1,0} + P_{2,0} L_{2,0}) / (L_{1,0} + L_{2,0}) = 1.6$ bar. Figure 4a shows the pig velocity, and Fig. 4b shows the upstream and downstream gas pressures. The linear undamped period of oscillation $\tau = 0.6$ s fits well with the calculated first period of 0.5 s of the nonlinear damped oscillation.

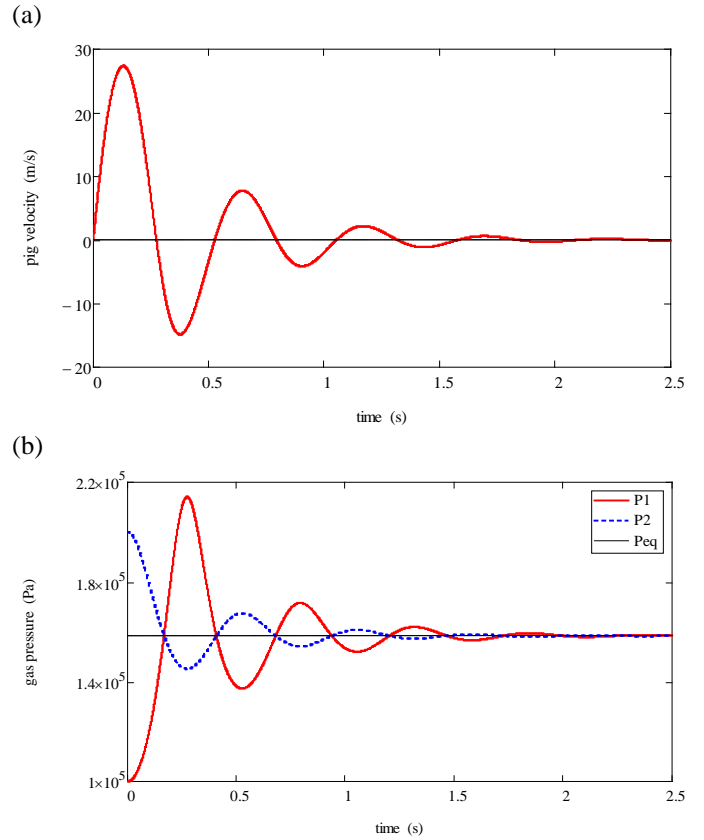


Fig. 4 Solid pig impact: (a) pig velocity versus time; (b) gas pressures versus time.

CONCLUSION

The pressure-driven propagation of a rigid body (liquid or solid) in a closed gas-filled pipe has been studied by means of basic models for which analytical solutions have been derived. The obtained solutions are used to predict maximum velocities, maximum pressures and maximum temperatures. The symbolic expressions reveal dimensionless parameters that fully characterize the problem. The solution’s sensitivity to these parameters can now be determined analytically. The symbolic solutions are easily implemented in scientific software and they can be used to verify numerical solutions.

ACKNOWLEDGMENT

The first author participates in the SLING (Sloshing of Liquefied Natural Gas) project which is funded by STW, MARIN, GTT, and eleven other companies and institutes. The second author is grateful for the support by the National Natural Science Foundation of China (No. 51478305), China Special Fund for Hydraulic Research in the Public Interest (No.

NOMENCLATURE

A	= cross-sectional conduit area (m^2)
a	= sonic speed in liquid (m/s)
a_{gas}	= sonic speed in gas (m/s)
c	= linear friction coefficient (kg/s)
D	= pipe diameter (m)
e	= exponential function
E_i	= exponential integral
E_n	= generalized exponential integral
F	= driving acceleration (m/s^2)
f	= Darcy-Weisbach friction coefficient
\mathbf{f}	= vector function
G	= driving acceleration (m/s^2)
g	= acceleration due to gravity (m/s^2)
K^*	= effective bulk modulus (Pa)
k	= spring stiffness (N/m)
L_{gas}	= length of gas pocket (m)
L_0	= length of liquid slug (m)
m	= mass of liquid slug or solid body (kg)
m_{gas}	= mass of gas pocket (kg)
n	= constant polytropic exponent
ODE	= ordinary differential equation
P	= absolute pressure (Pa)
P_{gas}	= absolute pressure of gas pocket (Pa)
$P_{R,0}$	= constant absolute reservoir pressure (Pa)
R	= specific gas constant ($m^2/(s^2 K)$)
S_B	= Bagnold number
S_M	= (Sam) Martin number
T	= absolute temperature (K)
t	= time (s)
V_{gas}	= volume of gas pocket (m^3)
v	= velocity of liquid slug or rigid body (m/s)
w	= width of slug front (m)
x_L	= total pipe length (m)
x_1	= axial position of slug front (m)
x_2	= axial position of slug tail (m)
\mathbf{y}	= vector of unknowns
Γ	= incomplete gamma function
θ	= angle of downward inclination of pipe (rad)
ξ	= small displacement (m)
ρ	= mass density of liquid (kg/m^3)
ρ_{gas}	= mass density of gas (kg/m^3)
τ	= period of oscillation (s)

Subscripts

eq	= equilibrium
max	= maximum
min	= minimum
0	= constant, initial value

REFERENCES

- [1] Bozkuş Z, Wiggert DC (1997) Liquid slug motion in a voided line. *Journal of Fluids and Structures* 11, 947-963.
- [2] Hou Q, Tijsseling AS, Bozkuş Z (2014) Dynamic force on an elbow caused by a traveling liquid slug. *ASME Journal of Pressure Vessel Technology* 136, art. no. 031302.
- [3] Tijsseling AS, Hou Q, Bozkuş Z (2016) An improved one-dimensional model for liquid slugs travelling in pipelines. *ASME Journal of Pressure Vessel Technology* 138, art. no. 011301.
- [4] Martin CS (1976) Entrapped air in pipelines. *BHRA Fluid Engineering, Proceedings of the Second International Conference on Pressure Surges, London, UK, Paper F2*, pp. 15-28.
- [5] Aktershev SP, Fedorov AV (1987) Increase in water-hammer pressure in a pipe in the presence of a localized volume of gas. *Journal of Applied Mechanics and Technical Physics* 28 (6), 899-903.
- [6] Hashimoto K, Imaeda M, Osayama A (1988) Transients of fluid lines containing an air pocket or liquid column. *Journal of Fluid Control* 18 (4), 38-54.
- [7] Aktershev SP, Petrov AP, Fedorov AV (1990) Effect of a gas cavity on a pressure surge in a hydraulic line. *Journal of Applied Mechanics and Technical Physics* 31 (3), 428-431.
- [8] Cabrera E, Abreu JM, Pérez R, Vela A (1992) Influence of liquid length variation in hydraulic transients. *ASCE Journal of Hydraulic Engineering* 118, 1639-1650. *Discussion and Closure*: 120, 661-666.
- [9] Tijsseling AS, Hou Q, Bozkuş Z (2015) Analytical expressions for liquid-column velocities in pipelines with entrapped gas. *Proceedings of the ASME Pressure Vessels and Piping Division Conference, Boston, USA, Paper PVP2015-45184*.
- [10] Tijsseling AS, Hou Q, Bozkuş Z (2016) Analytical and numerical solution for a rigid liquid-column moving in a pipe with fluctuating reservoir-head and venting entrapped-gas. *Proceedings of the ASME Pressure Vessels and Piping Division Conference, Vancouver, Canada, Paper PVP2016-63193*.
- [11] Bagnold RA (1939) Interim report on wave-pressure research. *Journal of The Institution of Civil Engineers, Vol. 12*, 201-226.
- [12] Brosset L, Ghidaglia JM, Guilcher PM, Le Tarnec L (2013) Generalized Bagnold model. *Proceedings of the 23rd International Offshore and Polar Engineering Conference, Anchorage, Alaska, USA, ISOPE, Vol. 3*, 209-223.
- [13] Guilcher PM, Jus Y, Couty N, Brosset L, Sclan YM, Le Touzé D (2014) 2D simulations of breaking wave impacts

on a flat rigid wall – Part 1: Influence of the wave shape. Proceedings of the 24th International Offshore and Polar Engineering Conference, Busan, Korea, ISOPE, Vol. 3, 232-245.

- [14] Abrahamsen BC, Faltinsen OM (2011) The effect of air leakage and heat exchange on the decay of entrapped air pocket slamming oscillations. *Physics of Fluids* 23, art. no. 1021077.
- [15] Abrahamsen BC, Faltinsen OM (2012) The natural frequency of the pressure oscillations inside a water-wave entrapped air pocket on a rigid wall. *Journal of Fluids and Structures* 35, 200-212.
- [16] Oh SH, Kwon SH, Chung JY (2009) A close look at air pocket evolution in flat impact. Proceedings of the 24th International Workshop on Water Waves and Floating Bodies, Zelenogorsk, Russia, pp. 19-22.
- [17] Park CW, Shin JY, Kwon SH, Chung JY, Lee SB, Yang YJ, Jung JH, Yoon HS (2012) A study on gap influence on slamming experiment. Proceedings of the ASME 31st International Conference on Ocean, Offshore and Arctic Engineering, Rio de Janeiro, Brazil, Vol. 4, pp. 509-512, Paper OMAE2012-83524.
- [18] Qu Q, Ji G, Liu P, Wen X, Agarwal RK (2017) Numerical study of evolution of air pockets during water impact of a flat-bottom structure. Proceedings of the 55th AIAA Aerospace Sciences Meeting, AIAA SciTech Forum, Grapevine, USA, Paper AIAA 2017-1649.
- [19] Vardy AE, Bloor MIG, Fox JA (1972) Capsular flow in pipelines. *Journal of Fluid Mechanics* 56, 49-59.
- [20] Weingarten JS, Chapman AJ, Walker WF (1984). An analysis of the motion of pigs through gas pipelines. *ASME Journal of Fluids Engineering* 106 (4), 374-379.
- [21] Kim DK, Cho SH, Park SS, Rho YW, Hui RY, Nguyen TT, Kim SB (2003) Verification of the theoretical model for analyzing dynamic behavior of the PIG from actual pigging. *KSME International Journal* 17 (9), 1349–1357.
- [22] Tolmasquim ST, Nieckele AO (2008) Design and control of pig operations through pipelines. *Journal of Petroleum Science and Engineering* 62 (3–4), 102-110.
- [23] Esmaeilzadeh F, Mowla D, Asemani M (2009) Mathematical modeling and simulation of pigging operation in gas and liquid pipelines. *Journal of Petroleum Science and Engineering* 69 (1–2), 100-106.
- [24] Botros KK, Golshan H (2010) Field validation of a dynamic model for an MFL ILI tool in gas pipelines. Proceedings of the ASME International Pipeline Conference, Calgary, Canada, Vol. 3, pp. 325-335, Paper IPC2010-31018.
- [25] Veilleux J-C, Shepherd JE (2017) Impulsively-generated pressure transients and strains in a cylindrical fluid-filled tube terminated by a converging section. Proceedings of the ASME Pressure Vessels and Piping Division Conference, Hawaii, USA, Paper PVP2017-65471.
- [26] Abreu JM, Cabrera E, García-Serra J, Izquierdo J (1991) Boundary between elastic and inelastic models in hydraulic

transients analysis with entrapped air pockets. IAHR, Proceedings of the 9th Round Table on Hydraulic Transients with Water Column Separation, Valencia, Spain, pp. 159–181.

- [27] Guarga R, Acosta A, Lorenzo E (1996) Dynamic compression of entrapped air pockets by elastic water columns. Proceedings of the 18th IAHR Symposium on Hydraulic Machinery and Cavitation (Editors E Cabrera, V Espert, F Martínez), Valencia, Spain, pp. 710-719; Dordrecht, The Netherlands: Kluwer Academic Publishers.
- [28] Chaiko MA, Brinckman (2002) Models for analysis of water hammer in piping with entrapped air. *ASME Journal of Fluids Engineering* 124, 194-204.
- [29] Epstein M (2008) A simple approach to the prediction of waterhammer transients in a pipe line with entrapped air. *Nuclear Engineering and Design* 238, 2182–2188.
- [30] Goyder H (2007) Gas waterhammer. Proceedings of the ASME Pressure Vessels and Piping Division Conference, San Antonio, USA, Paper PVP2007-26199, pp. 383-390.
- [31] Bozkuş Z, Baran Ö, Ger M (2004) Experimental and numerical analysis of transient liquid slug motion in a voided line. *ASME Journal of Pressure Vessel Technology* 126, 241-249.

APPENDIX A

The integrals in Eqs. (8) can be evaluated symbolically if one wishes to do so. For example, for $n = 1$,

$$\int_{x_{1,0}}^{x_1} \frac{e^{\frac{f}{D}x}}{x_L - x} dx = e^{\frac{f}{D}x_L} \left\{ \text{Ei} \left[\frac{f}{D}(x_{1,0} - x_L) \right] - \text{Ei} \left[\frac{f}{D}(x_1 - x_L) \right] \right\} \quad (\text{A1})$$

where Ei is the exponential integral. For $n \neq 1$, the integral

$$\int_{x_{1,0}}^{x_1} e^{\frac{f}{D}x} \left(\frac{1}{x_L - x} \right)^n dx \quad (\text{A2})$$

can be expressed in terms of the generalized exponential integral

$$E_n(u) := \int_1^{\infty} \frac{e^{-ux}}{x^n} dx = u^{n-1} \Gamma(1-n, u) = u^{n-1} \frac{1}{n-1} \left[\Gamma(2-n, u) - u^{1-n} e^{-u} \right] \quad (\text{A3})$$

where Γ is the incomplete gamma function. Note that $E_1(u) = -\text{Ei}(-u)$, $u > 0$. Transformations of variables and integrations by parts are needed to arrive at valid analytical expressions. It is therefore easier (and probably more accurate) to integrate Eqs. (8) numerically.

APPENDIX B

The extended Bagnold [12] model describes the frictionless motion of a liquid slug sandwiched between two entrapped gas pockets. The governing equations for a rigid slug are

$$\frac{dv}{dt} = \frac{P_2 - P_1}{\rho L_0} + g \sin \theta \quad (\text{B1})$$

$$\frac{dx_1}{dt} = v \quad (\text{B2})$$

$$L_1^n P_1 = L_{1,0}^n P_{1,0} \quad (\text{B3})$$

$$L_2^n P_2 = L_{2,0}^n P_{2,0} \quad (\text{B4})$$

where P_1 and P_2 are the absolute gas pressures, $L_1 = x_L - x_1$ and $L_2 = x_2 = x_1 - L_0$, as sketched in Fig. 2. Substitution of Eqs. (B3) and (B4) into Eq. (B1) gives

$$\frac{dv}{dt} = G(x_1) \quad (\text{B5})$$

where

$$G(x_1) = \left(\frac{L_0 - x_{1,0}}{L_0 - x_1} \right)^n \frac{P_{2,0}}{\rho L_0} - \left(\frac{x_L - x_{1,0}}{x_L - x_1} \right)^n \frac{P_{1,0}}{\rho L_0} + g \sin \theta \quad (\text{B6})$$

and $x_{1,0} = L_0 + L_{2,0}$.

The Eqs. (B2) and (B5) can be combined such that

$$\frac{dv^2}{dx_1} = 2G(x_1) \quad (\text{B7})$$

The solution is

$$v^2(x_1) - v^2(x_{1,0}) = 2 \int_{x_{1,0}}^{x_1} G(x) dx \quad (\text{B8})$$

For $n = 1$ this gives

$$v^2(x_1) - v^2(x_{1,0}) = \frac{2}{\rho L_0} \left[P_{2,0} (L_0 - x_{1,0}) \ln \left(\frac{L_0 - x_{1,0}}{L_0 - x_1} \right) - P_{1,0} (x_L - x_{1,0}) \ln \left(\frac{x_L - x_{1,0}}{x_L - x_1} \right) \right] + \rho g L_0 \sin \theta (x_1 - x_{1,0}) \quad (\text{B9a})$$

and for $n \neq 1$:

$$v^2(x_1) - v^2(x_{1,0}) = \frac{2}{\rho L_0} \left[\frac{P_{2,0}}{n-1} (L_0 - x_{1,0}) \left(\left(\frac{L_0 - x_{1,0}}{L_0 - x_1} \right)^{n-1} - 1 \right) - \frac{P_{1,0}}{n-1} (x_L - x_{1,0}) \left(\left(\frac{x_L - x_{1,0}}{x_L - x_1} \right)^{n-1} - 1 \right) + \rho g L_0 \sin \theta (x_1 - x_{1,0}) \right] \quad (\text{B9b})$$

The functions $v(x_1) = +\sqrt{v^2(x_1)}$ and $v(x_1) = -\sqrt{v^2(x_1)}$ together describe a symmetric closed curve. The functions are defined between $x_{1,\min}$ and $x_{1,\max}$ (the turning points), the values of which are the two zeros of the function $v^2(x_1)$. For $v^2(x_{1,0}) = 0$ it is obvious that $x_{1,\min} = x_{1,0}$. The maximum displacement $x_{1,\max}$ [the non-trivial root of $v^2(x_1)$ when starting from rest] can easily be determined numerically. The maximum gas pressure $P_{1,\max}$ follows then from $L_{1,\min} = x_L - x_{1,\max}$ and Eq. (3), and the corresponding maximum temperature from Eq. (13).